

## Extraterrestrial safety: On the management of Artemis Mission

Ronald H. Freeman, PhD

Editor-in-Chief, Journal of Space Operations & Communicator

[ronaldhoracefreeman@gmail.com](mailto:ronaldhoracefreeman@gmail.com)

**Abstract,**This paper explores current strategies needed to protect and monitor the health of Artemis missions involving astronauts, autonomous rovers, mobile habitats, ISRU equipment and facilities. Exposed to solar wind plasma, GCRs and secondary radiation due to the lack of a magnetosphere or a dense atmosphere. sparse regional mini-magnetospheres don't spare the intense space weathering of the Moon's regolith covered surface. Nor exposure risk to levitated dust particles of the Moon safeguards mission operations. Levitated dust particles settle and accumulate on hardware which may result in potential degradation of radiative heat transfer and optical components through the fouling of surfaces, visibility reduction during extravehicular activities, and dust contamination of equipment and prevention of effective sealing.

**Keywords:** radiation shielding materials, lunar dust particle removal

### I. Introduction

In establishing Artemis Base Camp on the Moon, it may be best to anticipate its environmental conditions and what impacts the installed cyber-physical structures may suffer. First there is no lunar atmosphere or contiguous magnetosphere, so, interplanetary galactic cosmic rays, solar winds, cosmic rays, and secondary radiation, resulting in fluxes of both ultraviolet and ionizing radiation. Both the Earth and spacecraft of LEO, including ISS, are protected from ionizing radiation due to the protective effects of the Earth's atmosphere and geomagnetosphere. Beyond the Earth's geomagnetosphere, however, the space radiation environment is not only unmitigated but also characterized by a different types of radiation in addition to the electromagnetic—namely, galactic cosmic radiation (i.e., high energy protons and heavier ions traveling through space at relativistic speeds) and moderate-to-high energy protons released from the sun during solar particle events (SPEs) .

	Gravity (g)	Temperature range (°C)	UV range (nm)	Ionizing radiation dose (average, mGy/year)	Dominant ionizing radiations	Atmosphere (hPa and dominant gases)
Earth	1	-90 to +60	>300	~1	muons, neutrons, electrons	1013 at sea level (N <sub>2</sub> , O <sub>2</sub> )
ISS in LEO	0	-160 to +120	>10	~240	electrons, protons	10 <sup>-6</sup> – 10 <sup>-5</sup>
Moon	0.16	-180 to +130	>10	~100	GCRs, SEPs, neutrons	10 <sup>-12</sup> – 10 <sup>-8</sup>
Mars	0.38	-150 to +30	>190	~90	GCRs, SEPs, neutrons	0.6 – 1.2 (CO <sub>2</sub> , N <sub>2</sub> , Ar)

Figure 1 . Comparison of some environmental factors on the surface of Earth, the Moon and Mars, and outside the ISS in low Earth orbit. Adapted from Cottin et al. (2017) with additions from Hassler et al. (2014), Reitz et al. (2012), Dachev et al. (2017), Rabbow et al. (2017).

The lunar environment is instead controlled by the flux of photons and ions from the solar wind, cosmic rays, and galactic cosmic rays. The lunar surface is composed of rocks and granular material with grains and dust particles ranging in size from a few centimeters down to a few nanometers. This granular material is expected to be electrostatically charged due to the incident plasma and to the UV from the sun, which releases photoelectrons from the surface of the material. The plasma and photon fluxes bathing the moon produce a complex electrostatic environment. On the sunlit side, photoelectric charging by solar UV photons dominates. The emission of photoelectrons leaves the surface positively charged to a potential of about 5 to 10 V [1]. On the dark side, plasma electrons dominate and the surface becomes negatively charged to a negative potential of the order of the electron temperature, about -50 to -100 V [2]. The moon is essentially a charged body in plasma, creating a screening effect in the plasma with a characteristic distance or Debye length of the order of meters on the lunar dayside and of the order of kilometers on the dark side.

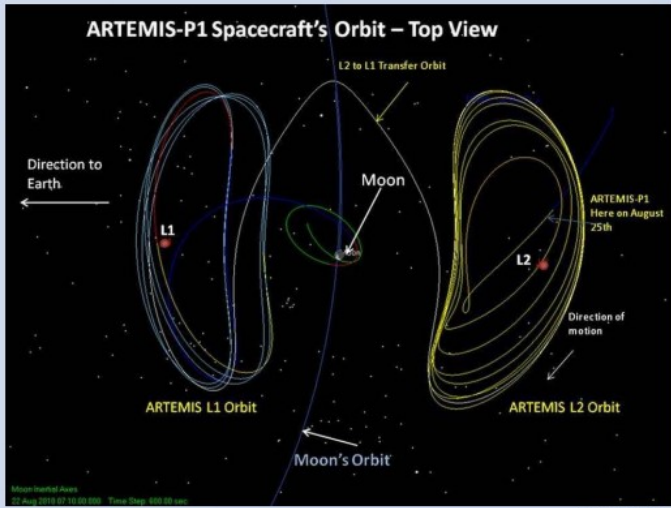
The lunar surface is directly exposed to solar wind plasma due to the Moon's lack of a magnetosphere or a dense atmosphere. This results in intense space weathering of the regolith covered surface [3]. When solar wind hits the surface, a fraction of it is reflected as protons [4] and as neutral hydrogen atoms [5]. The surface of the Moon is baldly exposed to cosmic rays and solar flares, and some of that radiation is very hard to stop with shielding. Furthermore, when cosmic rays hit the ground, they produce a dangerous spray of secondary particles. To carefully measure and map the Moon's radiation environment, NASA developed Lunar Reconnaissance Orbiter (LRO), a robotic probe to orbit the Moon, in 2008. One of the instruments onboard LRO is the Cosmic Ray Telescope for the Effects of Radiation (CRaTER). The other radiation-sensing instrument on LRO, the Lunar Exploration Neutron Detector (LEND), detects neutron radiation emanating from the lunar surface and measure how energetic those neutrons are [6]. Recent solar conditions indicate a persistent decline in solar activity, during which fluxes of galactic cosmic rays (GCRs) increase, thus presenting a hazard for long-term space missions.



## Electrostatic Charging of the Lunar Regolith

NASA Kennedy Space Center

- GCR particle radiation can generate deep dielectric charging down to a depth of ~1 m.
- Since the regolith has a very low electrical conductivity, electrostatic discharges can take place through the regolith.
- NASA's *Acceleration Reconnection Turbulence and Electrodynamics of the Moon's Interaction with the Sun* (ARTEMIS) mission, launched in 2010, is measuring the solar radiation incident on the Moon as it moves in and out the Earth's magnetic field.
- Winslow *et al* are applying ARTEMIS data to a deep dielectric charging model developed by Jordan *et al.* to estimate the subsurface electric field strength and dielectric breakdown.
- GCRs can also alter the chemical composition of the regolith



Moon's Orbital Axes  
07 Aug 2010 07:10:00 UTC Time Step: 000:00:00

NASA Image

- Winslow R M *et al* 2015 Lunar surface charging and possible dielectric breakdown in the regolith during two strong SEP events *46<sup>th</sup> Lunar and Planetary Science Conference* 1261
- Jordan A P Stubbs T J Wilson J K Schwadron N A and Spence H E 2015 *J. Geophys. Res.* **120** 210-225

Figure 2.,

The combination of small dust particles (between 60 and 80  $\mu\text{m}$  [7], electric potentials [8], plus micrometeorites can lead to lunar regolith being levitated [9]. Levitated dust particles may settle and accumulate on hardware which may result in potential degradation of radiative heat transfer and optical components through the fouling of surfaces, visibility reduction during extravehicular activities (EVAs), dust contamination of equipment and prevention of effective sealing [10].

Lunar dust is a ubiquitous problem on the Moon due to high particle angularity imparting high abrasiveness on seals, optical surfaces, thermal surfaces and, for human missions, deleterious physiological effects. Fine-grained lunar dust is levitated by solar ultraviolet radiation during the day and by solar wind flux during the night [11].

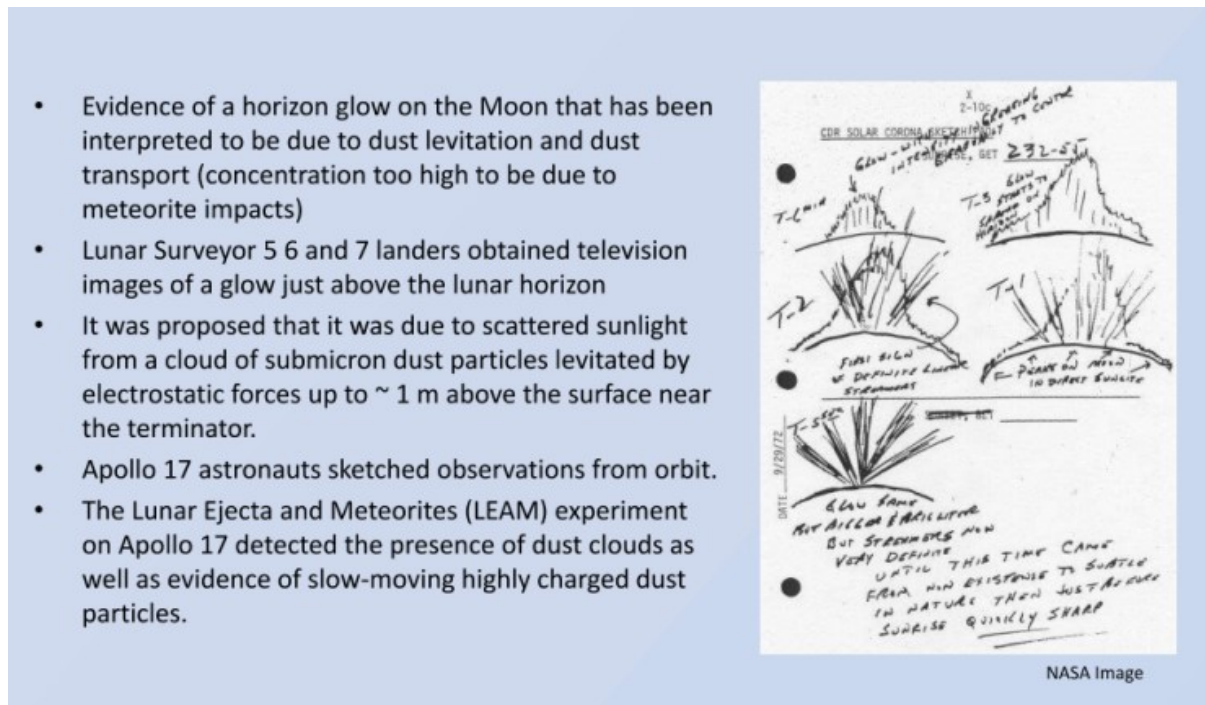


Figure 3.

Registration of dust particle dynamics above the lunar surface was first performed using the Lunar Ejecta and Meteorite (LEAM) experiment deployed on the lunar surface by astronauts of the Apollo 17 mission [12]. The LEAM instrument had several detectors for recording high-speed ( $1 < v < 25 \text{ km/s}^{-1}$ ) micrometeorites. However, one of the detectors was able to register low-velocity particles. The data from this detector were the data that gave unexpected results about rather high fluxes of low-velocity ( $v \sim 100\text{--}1000 \text{ m/s}^{-1}$ ) particles, the charge of which was usually  $Q > 10^{-12} \text{ C}$  (or  $> 6 \times 10^6$  electron charges). During the operation of the instrument, the maximum counting rate of the detectors was observed in the region of the terminator. Figure 4 shows the number of registrations of dust particles in a 3-hour interval (counting rate), summed up over 22 lunar days. This graph shows an increase in the count rate of dust grains for several hours before and after crossing the terminator, and the most significant increase in the count rate was in the region of sunrise. However, subsequent detailed analysis of the data cast doubt on this conclusion [13].

The unusual ability of lunar dust to penetrate the seals of sealed units and to “stick” to various surfaces can be considered in terms of the dynamic properties of lunar dust particles levitating above the surface. The point is that levitating submicron and micron particles, when interacting with a surface, can manifest as more than “impactors.” By levitating, dust particles can rotate rapidly. Estimates made by [15] showed that the speed of proper rotation of levitating micron and submicron particles on the illuminated side of the Moon can range from several thousand to tens of millions of revolutions per second. Furthermore, considering the impact origin of such particles, their shapes are extremely irregular and often pointed [16]. All this suggests that such rapidly rotating particles resemble eastern

shuriken (or ninja stars) with great destructive power [17]. Apparently, this feature, in combination with the existing electrostatic charge, explains the amazing ability of lunar dust to aggressively affect the surfaces of the sensitive systems of the instruments and lander and to penetrate through hermetic seals.

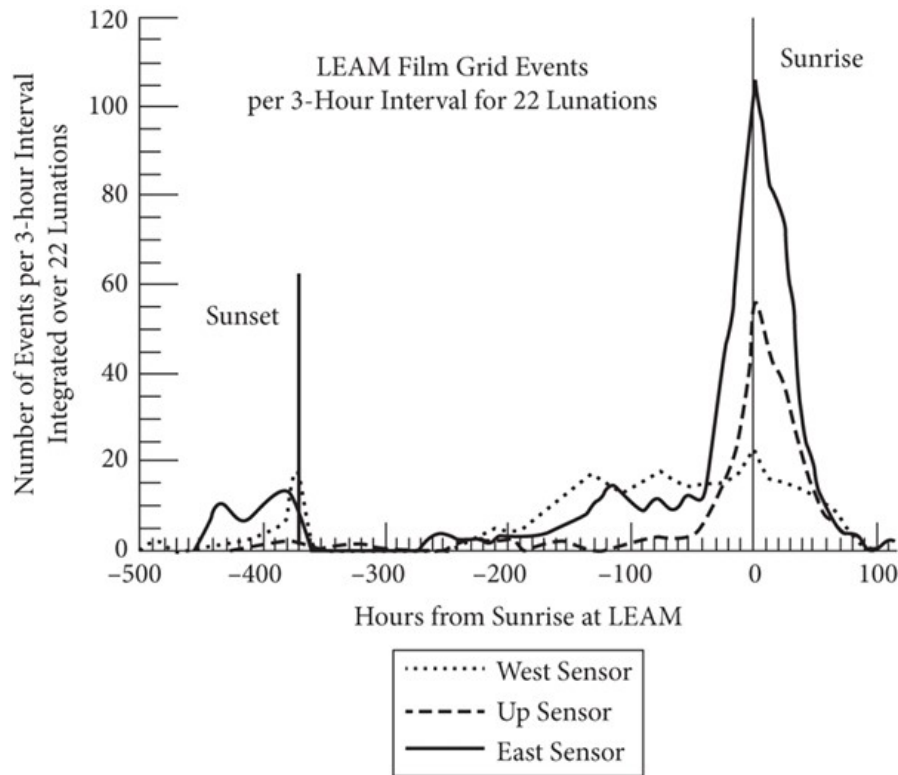


Figure 4 . The number of registrations of dust particles in a 3-hour interval of measurements above the lunar surface by the LEAM instrument. The data were integrated over 22 lunar days [14].

The model of levitation of dust particles under the action of electrostatic forces was developed by [18]. The essence of the model is as follows. Solar electromagnetic radiations, as well as flows of interplanetary plasma, ions, and electrons of the solar wind, acting on the regolith, create currents through the surface. Moreover, for the illuminated side of the Moon under solar wind conditions, the photocurrent density  $J_{ph}$  from the action of solar UV and soft X-radiation is usually an order of magnitude higher than the currents of electrons  $J_e$  and ions  $J_i$  of the solar wind, or  $|J_{ph}| \gg |J_e| \gg |J_i|$ , as well as secondary radiation electrons on the lunar surface [19]. These currents depend on the surface potential, and in the equilibrium state at the formed surface potential, their sum is close to zero [20]. Considering that the surface of the regolith is close to a dielectric [21] the acquired surface potential can be maintained for a long time [22]. In this case, a double (plasma) layer with an electric field  $E$  appears between the charged surface of the Moon and the surrounding quasineutral plasma. The characteristic height of this layer is of the order of the Debye length, which corresponds to several tens of centimeters. The Coulomb force  $qE$ , the gravitational force  $mgL$  ( $m$  is the mass of the particle,  $gL$  is the acceleration of gravity on the Moon), and the van der Waals adhesion forces  $F_c$  act on dust particles lying on the surface of the Moon that have received an electric charge  $q$ . If the Coulomb repulsive force exceeds the sum of the forces holding a dust particle on the surface,  $qE > mgL + F_c$ , the particle is detached from the surface and levitates in the near-surface electric field. The condition for particle levitation is the approximate equality of the electric and gravitational forces  $qE \approx mgL$ . The concept of dust particles levitating over the surface of the regolith was proposed in [23] and [24]. Depending on the conditions in which the lunar surface is located, the sign and magnitude of the surface potential, as well as the values of the electric field, can change significantly. This is a general picture of the formation of the potential of the regolith surface, the near-surface electric field, and the conditions for the dynamics of dust particles.

Lunar regolith has increasing abundances of agglutinate glasses and nanophase metallic iron content with decreasing size with a Gaussian average size of  $3.0 \mu\text{m}$  [25]. Nanophase iron Fe0 in lunar regolith appear as  $\sim 10 \text{ nm}$  diameter inclusions within glasses produced by microtektite bombardment of the lunar surface (Keller & Klemmet 2001).

This nanophase iron significantly increases the oxidative reactivity of regolith due to the production of hydroxyl radicals through Fenton reactions with iron oxides [26].

## II. Method and Results

Extending the technical paper presentation “Artemis Base Camp: Resilience Engineering to Enable Lunar Surface Operations” at the “Lunar Surface Science Workshop XIV: Heliophysics Applications Enabling and Enabled by Human Exploration of the Lunar Surface” (virtual, February 17, 2022), the author performed a literature review of current mitigation strategies for the safety of future deep space missions as related to space-based hardware and the cyber-physical functions therein.

### Advanced radiation shielding materials

The Exploration Systems Architecture Study (ESAS) identified baseline elements of the Constellation Program that enables human exploration beyond low-earth orbit. The Constellation Program provides the infrastructure to implement the Vision for Space Exploration. The ESAS team also evaluated technologies that could reduce the cost, schedule and risk of implementing the architecture. Two technology areas, designated as ESAS References 1A (lightweight structures) and 9D (low temperature mechanisms) were deemed crucial to reduce the mass and risk of various elements of the architecture. [27].

Table 3 Lightweight Structures Challenges/Risks and Technology Solutions

Constellation Application	Challenges/risks to achieve reduce mass	Technology solutions	Technology metrics
CEV CM	MMOD, Structural Reliability, Radiation Protection	Multifunctional Structures, Advance Materials, Radiation Shielding Materials, Composite (Adv. Metals) Reliability	Structural Efficiency, GCR Dose, MMOD Impact Size And Velocity Survival For Areal Mass
Cryotanks (CLV, Landers)	Improved Manufacturing, Structural Reliability	Advanced Manufacturing Methods (FSW), Multifunctional Structures, Advance Materials	Structural Efficiency, Durability
Lunar Landers	MMOD, Structural Reliability, Radiation Protection, Increased Operational Volume	Multifunctional Structures, Advance Materials, Radiation Shielding Materials, Composite (Adv. Metals) Reliability, Inflatable Structures	Structural Efficiency, GCR Dose, MMOD Impact Size And Velocity Survival For Areal Mass, Packaging Density
Lunar Habitats	MMOD, Structural Reliability, Radiation Protection, Increased Operational Volume	Multifunctional Structures, Advance Materials, Radiation Shielding Materials, Composite (Adv. Metals) Reliability, Inflatable Structures	Structural Efficiency, GCR Dose, MMOD Impact Size And Velocity Survival For Areal Mass, Packaging Density

### Radiation Shielding Materials

Development Radiation effectiveness will be considered as an integral part of the design of the total material system comprising the structural components. A separate materials development program will not be supported by this activity because it is realized that radiation effectiveness is one of many figures of merit to aid in the selection and evaluation of multifunctional structural shielding. However as part of this program a survey of existing materials (TRL 3 and above) will be performed to estimate the radiation effectiveness against solar proton events, galactic cosmic radiation, and the appropriate reference design environments. Promising materials currently under development may be selected for continued development within this task based upon need and ability to meet requirements compared with other systems of similar TRL.

### Multifunctional Structures

This task is to develop multifunctional structures technology for application to primary structure of the lunar lander crew habitat and lunar surface habitats with relevant technology made available to CEV (crew exploration vehicle\_Orion) and CLV (crew exploration vehicle\_Ares I) elements. Multifunctional structure in this project is defined as a structural system that incorporates material systems and structural configurations to combine the functions of required structural performance, radiation protection, MMOD (micrometeoroid and orbital debris) protection, thermal control, and structural health monitoring within one structural system. The goal of this task is to develop a primary structural system with reduced mass compared to the current practices of combined structural and parasitic systems required for the same type of performance and to demonstrate this system in a structural subcomponent demonstration.

#### Lunar Lander Structures Technology

The major mechanical/structural constraints on the lander are the mass delivery capability of the CaLV (cargo launch vehicle\_Ares V), the volume of the CaLV shroud, and the descent/ascent requirement of a pressurized volume for the crew. These constraints are further exacerbated by the harsh radiation, micrometeoroid, thermal and abrasive dust environment on the lunar surface. A key component of the LL (lunar lander) is the vehicle pressure. The initial sortie missions are likely to utilize either a rigid metallic or polymer matrix composite (PMC) pressure shell. The material system selection is not based solely on mechanical and thermal loads, but also on MMOD and radiation considerations. NASA's CEV Smart Buyer study [28] also identified the mass savings of composites for the Crew Module pressure vessel. Efforts within NASA are now underway to develop a composite CM design and to assess the durability of composites that undergo hypervelocity (simulated MMOD) impacts.

Utilization of regolith on the roof and walls of a habitat to shield the internal volume from galactic cosmic radiation (GCR) particles is of high interest for long duration outpost missions. A thorough study of shielding using regolith is presented in [29]. An average regolith density of 1.5 g/cm<sup>3</sup> is used to estimate the required depth of regolith needed for various levels of shielding. As indicated in [30], a 3 meter thick regolith shield produces a dead load of 8.3 KpA (1.2) psi. Again, this gravity load could be used to offset pressure induced loads for inflatable habitats if properly designed.

Energetic ion beam experiments with major space radiation elements, 1 H, 4 He, 16O, 28Si and 56Fe, have been conducted to investigate the radiation shielding properties of composite materials. These materials are expected to be used for parts and fixtures of space vehicles due to both their mechanical strength and their space radiation shielding capabilities. Low Z materials containing hydrogen are effective for shielding protons and heavy ions due to their high stopping power and large fragmentation cross section per unit mass. The stopping power of the composite materials used in this work is intermediate between that of aluminum and polyethylene, which are typical structural and shielding materials used in space. The total charge-changing cross sections per unit mass,  $\sigma_{UM}$ , of the composite materials are 1.3–1.8 times larger than that of aluminum. By replacing conventional aluminum used for spacecraft with commercially available composite (carbon fiber / polyether ether ketone), it is expected that the shielding effect is increased by ~17%. The utilization of composite materials will help mitigate the space radiation hazard on future deep space missions [31].

The composite materials are made of resins, reinforced to enhance mechanical strength. The resin is an organic polymer such as polyether ether ketone (PEEK), polyimide (PI) and polypropylene (PP), which is selected based on its the chemical and thermal properties. Carbon fiber (CF) or silicon carbide is used for reinforcement. The selection of appropriate resins and reinforcements allows the composite materials to be more shock- and heat-resistant than resin and reinforcement alone. Composite materials are already used in automobiles, airplanes and spacecraft because of their low density and high mechanical strength [32]. Composite materials contribute not only to structural strength in spacecraft but also to radiation shielding by their relatively higher stopping power and a larger nuclear fragmentation cross section per unit mass compared to Al [33]. To evaluate the shielding efficiencies of target materials, the materials were irradiated with protons and heavy ion beams representing major components of the GCR in the biological irradiation room of HIMAC (Heavy Ion Medical Accelerator in Chiba) of QST, Japan. Table 2 lists the beam energies and calculated LET values in water. We note that these energies are the maximum available for each ion at the HIMAC, which are somewhat lower than the mean energy of the corresponding GCR particles (~1 GeV/n). The ranges of beams in the target materials are listed in Table 3.

**Table 2**  
Energy and calculated LET in water of each beam.

Ion	Energy (MeV/n)	LET in water (keV/μm)
<sup>1</sup> H	228	0.4
<sup>4</sup> He	145	2.3
<sup>16</sup> O	380	20.0
<sup>28</sup> Si	440	56.9
<sup>56</sup> Fe	410	199.5

**Table 1**  
Target materials used in our experiments and their physical parameters.

Material <sup>a</sup>	Density (g/cm <sup>3</sup> )	Size of sample (cm × cm)	Resin <sup>b</sup>	Reinforcement <sup>c</sup>	Resin fraction (wt%)	Z <sub>T</sub> /A <sub>T</sub>	A <sub>T</sub> <sup>-1/3</sup>
Al	2.7	10 × 10	—	—	—	0.481	0.333
PE	0.94	10 × 10	—	—	—	0.570	0.598
PP SiC20 <sup>b</sup>	1.36	10 × 10	PP	SiC	53	0.537	0.515
PP SiC40 <sup>b</sup>	1.81	10 × 10	PP	SiC	30	0.520	0.462
PP C	1.17	10 × 10	PP	C	62	0.543	0.547
PE SiC	1.36	10 × 10	PE	SiC	53	0.537	0.516
CF/PI	1.43	6 × 6	PI	CF	70	0.511	0.466
CF/PEEK	1.62	5.5 × 5.5	PEEK	CF	33	0.508	0.434
CF/PP	1.31	10 × 10	PP	CF	33	0.523	0.502
CF/Epoxy	1.57	10 × 10	Epoxy <sup>d</sup>	CF	34	0.510	0.464

<sup>a</sup> PE, polyethylene; PI, polyimide; CF, carbon fiber; PEEK, polyether ether ketone; PP, polypropylene.

<sup>b</sup> SiC20 and SiC40, the numbers indicate percent volume of SiC in the composite material.

<sup>c</sup> Composition of the epoxy material is not publicly available. Therefore, Z<sub>T</sub> and A<sub>T</sub> of CF/Epoxy were estimated from its mass and density.

**Table. 3**  
Calculated range of each beam in each target material. CF/PI, CF/PEEK and CF/PP were not tested with <sup>1</sup>H, <sup>4</sup>He and <sup>16</sup>O beams.

Material	Range (mm)				
	<sup>1</sup> H 228 MeV	<sup>4</sup> He 145 MeV/n	<sup>16</sup> O 380 MeV/n	<sup>28</sup> Si 440 MeV/n	<sup>56</sup> Fe 410 MeV/n
Al	153.1	70.1	90.0	64.6	34.4
PE	326.2	149.5	193.0	138.8	73.9
PP	249.4	114.5	147.3	105.9	56.2
SiC20					
PP	198.0	91.3	116.7	84.0	44.7
SiC40					
PP C	276.5	127.2	163.9	118.0	62.6
PE SiC	248.8	113.9	146.3	105.6	56.2
CF/PI	—	—	—	104.6	55.7
CF/ PEEK	—	—	—	92.6	49.3
CF/PP	—	—	—	110.4	58.8

Radiation shielding properties of composite materials compared favorably to conventional materials of polyethylene as a shielding material and aluminum as a structural material in spacecraft. The composite materials had shielding efficiency intermediate between that of polyethylene and aluminum: >30% higher shielding efficiency than aluminum and <30% lower than polyethylene. By using a commercially available composite, CF/PEEK, for the HTV module structure, the effective dose equivalent due to galactic cosmic ray particles was found to be comparable to that with the aluminum HTV module despite its small mass by a factor of their density ratio of 1.67. A 35–70% larger CF/PEEK fragmentation cross section per unit mass provides effective radiation shielding. The use of composite materials in place of aluminum in spacecraft is a promising option for mitigation of space radiation exposure.

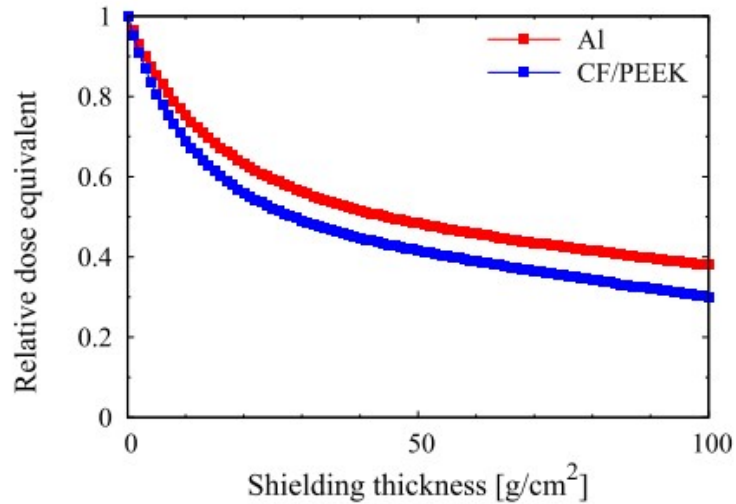


Fig. 9. Normalized effective dose equivalents as a function of shielding thickness of Al and CF/PEEK.

Additionally, Anti-radiation nanostructures solutions create an anti-radiation effect achieved with suitable nanostructures, reduced density ( $d \leq 1.7 \text{ g cm}^{-3}$ ) compared to traditional lead-based protective anti-radiation suits. Furthermore, it is resistant to thermal cycling resistant to high energy radiation (dosage  $\geq 50 \text{ MRad}$ ). Boron nitride nanotubes (BNNTs) offer similar qualities as carbon nanotubes, plus additional traits, including high heat resistance together with the ability to block radiation. Multilayer composite structures provide high neutron shielding efficiency. By alternating high density polyethylene/ hexagonal boron (HDPE/hBN) with low density polyethylene (LDPE) layers, the former with a percentage of transmitted neutrons of only 4.16%. Neutron shielding results from neutron scattering and absorption. hBN with high thermal conductivity [34].

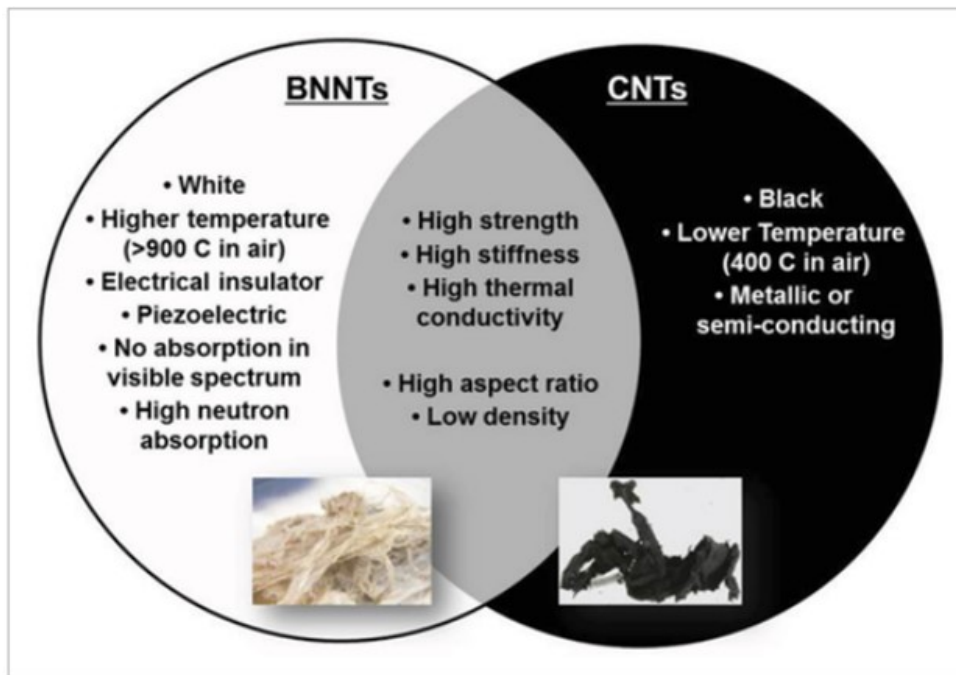


Figure 10

Boron Nitride Nanotubes are nano size hollow tubes formed by Boron and Nitrogen atoms. BNNTs structure is similar to Carbon Nanotubes (CNTs) where each C–C bonds is replaced by B–N bond with almost identical bond length. Although this similarity suggests that BNNTs properties is similar to CNTs but there are differences which makes BNNTs superior choice for specific application including radiation shielding and organic photovoltaic packaging [35]. Apart from replacing Carbon atoms with Boron and Nitrogen atoms which is main reason for BNNTs radiation shielding capability; CNTs may be semiconductor or metallic mainly depending on nanotubes chirality (based on chirality, Nanotubes can be categorized into three groups of Armchair, Zig Zag and Chiral) while BNNTs has a specific band gap of 5.0–6.0 eV [36]. Also BNNTs offer better thermal stability, chemical stability and higher thermal conductivity compared to CNTs while it possesses almost similar mechanical properties [37]. One of the interesting characteristics of BNNTs for space application is that it offers both mechanical support and radiation shielding capability which makes it suitable to be used in structural materials of space crafts or even astronauts suits. The radiation shielding of BNNTs is mainly relies on B10 capability in capturing harmful neutrons due to its large neutron capture cross section while Nitrogen is also effective shielding component (with much less role comparing to B10).

### **Lunar Dust Particle Removal**

In addition to mechanical forces (i.e., from rover wheels, astronaut boots, and rocket engine blast) static electric effects (from UV photo-ionization and/or triboelectric charging) are likely to be the major contributors to the motion of dust particles. If fine regolith particles are deposited on a surface, then surface energy related (e.g., van der Waals) adhesion forces, and static-electric-image forces are likely to be the strongest contributors to adhesion. The typical charge on particles coming from a lunar surface existing at a nearly uniform potential is expected to vary directly with the particle size. On the other hand, electrically levitated dust particles may attain net charges (from UV photo-ionization and neutralization by capture of electrons from the plasma sheath) which depend on the square of the particle size. Considerable uncertainty exists in estimates of the magnitude of surface-energy-related adhesive forces because the lunar environment may allow effective surface energies to be significantly higher than are typically observed in a terrestrial laboratory atmosphere where adsorbed gas molecules can lower the effective surface energy. A very dilute levitated layer of fine charged dust particles is likely in motion above the lunar surface and will deposit dust on any surface encountered, suggesting that even surfaces not in contact with the lunar soil, and far from man-made disturbances, will likely acquire layers of dust over time [38]. Since minerals comprising regolith are insulators, and there is no liquid water present, lunar surface is essentially nonconductive. This means charges produced on the surface will equilibrate with the external environment and are not conducted to an interior “ground” potential as might occur on earth. Charging of lunar dust particles can come from several sources (and, with no atmosphere, isolated non-conducting regolith particles can maintain a charge once acquired). Photoelectric ionization (from solar UV) on the lit side, and solar-wind electrons on the dark side (in equilibrium with any resulting near-surface plasmas) will result in a nearly uniform surface potential—positive or negative, on the sunlight side or dark side, respectively [39]. The electric field near a large charged surface (like a nearly uniformly charged lunar surface) decreases very slowly with distance away from the surface. Likewise, the static-electric force on a charged particle in such a field varies slowly with distance. Thus, electrostatic forces have the potential to contribute both as long-range forces affecting motion of fine particles and as short-range forces affecting their adhesion/cohesion, depending on the net charge on a particle and on the surface charge-density near a contact point [40].

A wide variety of cleaning methods exist for removing particles and other contaminants from surfaces. The microelectronics industry, in particular, is especially concerned with removing particles as fine as sub-micron-size from surfaces of silicon. Mitigation techniques identified as having potential for significant benefit included multilevel or multilayer barriers to prevent dust intrusion, electromagnetic “shields” and specialized coatings on surfaces to minimize dust accumulation, and a variety of approaches to remove dust once it is deposited on surfaces. Removal of particles from a surface requires methods (1) to deliver sufficient force to particles to dislodge them from the surface (e.g., overcome surface energy or electrostatic adhesion forces) and (2) to transport detached particles far enough away from the surface that they do not immediately redeposit. Mechanical vibration requires high frequencies in order to couple to the resonant frequency of attached particles—thus, ultra-sonic baths in liquids have proven effective at fine particle removal. Liquid immersion is not practical for most lunar situations. Also, direct mechanical (i.e., contact) vibration may not be practical for many configurations. A non-contacting electromagnetic “brush” with oscillating EM fields may offer a removal method applicable to a lunar environment, but such a device has yet to be demonstrated to be effective. Mechanical wiping or brushing of surfaces can deliver

sufficient force to dislodge particles, but can also cause serious damage to delicate surfaces due to scratching (especially if the particles are hard and angular, like lunar regolith fines). Removable soft, thin films, which can be either mechanically applied, or sprayed on, and pulled off offer an attractive alternative method of removing dust with minimal displacement along the surface (and thus minimal scratching) [41].

NASA's Artemis program will develop extensive resources on the Moon starting in 2024 and will require advanced technologies to enable a sustained lunar presence. Mitigation of lunar dust adhesion will be central to these efforts and to Artemis's success. A team at NASA/Jet Propulsion Laboratory (JPL) and Colorado University (CU), Boulder is developing new electron beam technology and a tool called a "Moon duster," which can be used to remove dust on sensitive surfaces of hardware and spacesuits on the Moon. Unlike other technologies that require incorporating a complex design of active embedded layers on the surface to be cleaned, the Moon duster is a standalone, hand-held electron beam device that can be potentially used on any dust-covered space hardware on the Moon. When an electron beam or UV field is applied to a micro-cavity formed in a pile of dust, the induced secondary electrons or photoelectrons are collected by the surrounding dust particles, resulting in a substantial negative charge buildup on the dust particles' surfaces. The repulsive force between these negatively charged dust particles ejects them off the surface [42].

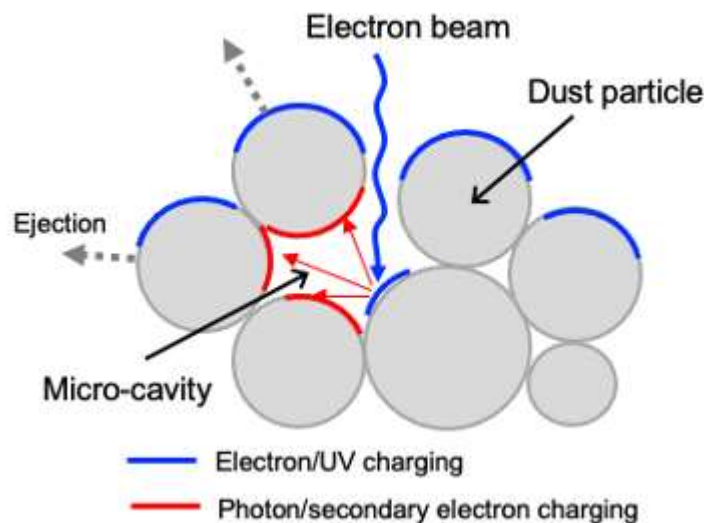


Figure 11. Dust charging and releasing mechanisms.

### III. Conclusion

Beyond the Earth, International Space Station, and surrounding orbits, space environment contrasts significantly different that in the deep space weather has nothing to filter or deflect galactic or solar radiative high-energy particle fluxes and micrometeorites to ravage the Moon. Dielectric discharging lunar surface deep down to 1 m results in regolith breakup and causes abundant dust particle levitation. The risk to hardware of autonomous systems and robotics deployed in lunar orbit (e.g. orbiters, cubesats) as well as lunar surface (e.g. landers, rovers) and their respective instruments results from ubiquitous high-energy GCR-/ SEP- particles and from levitated, highly angulated dust particles in their environs. Composite shielding materials such as polyether ether ketone (PEEK) and boron nitrides nanotubes, test more favorably than the traditional aluminum materials used for ISS. Composite materials of low atomic number materials containing hydrogen are also effective for shielding protons and heavy ions due to their high stopping power and large fragmentation cross section per unit mass.

Electrostatic forces have the potential to contribute both as long-range forces affecting motion of fine particles and as short-range forces affecting their adhesion/cohesion spacecraft and their respective instruments. Cleaning materials include multilevel or multilayer barriers to prevent dust intrusion, electromagnetic "shields" and

specialized coatings on surfaces to minimize dust accumulation, and a variety of approaches to remove dust once it is deposited on surfaces. Alternatively, ultra-sonic baths in liquids have proven effective at fine particle removal due to their high frequencies that couple to the resonant frequency of attached particles.

## References

- [1]. Manka, R. (1973). Plasma and potential at the lunar surface. *Photon and Particle Interactions with Surfaces in Space*, R.J.L Gard, Ed., Springer, NY, 347-361.
- [2]. Halekas, J., Mitchell, R., Lin, L., Hood, M., & Binder, A. (2002). Evidence for negative charging of the lunar surface in shadow. *Geophys. Res. Lett.* 29, 1436.
- [3]. Hapke, B. (2001) Space weathering from Mercury to the asteroid belt. *J. Geophys. Res.*, 106, 10039–10073.
- [4]. Holmström, M., Wieser, M., Barabash, S., Futaana, Y., Bhardwaj, A. (2010). Dynamics of solar wind protons reflected by the Moon. *J Geophys Res* 115,06206.
- [5]. McComas, D., Allegrini, F., Bochsler, P., Frisch, P., Funsten, H., Gruntman, M., & Schwadron, N. (2009). Lunar backscatter and neutralization of the solar wind: First observations of neutral atoms from the Moon. *Geophysical Research Letters*, 36(12).
- [6]. Robot Moonship To Test Radiation For Future Human Visit. (September 8, 2005). ScienceBlog.com
- [7]. McKay, D., Heiken, G., Basu, A., Blanford, G., Simon, S., Reedy, R., French, B., Papike, J. (1991). The lunar regolith. In: Heiken, G. Vaniman, D., French, B.(Eds.), *Lunar Sourcebook*. Cambridge University Press, Cambridge (Chapter 6).
- [8]. Pirich, R., Weir, J., Leyble, D., Chu, S., & DiGiuseppe, M. (2010). Effects of the Lunar Environment on Protective Coatings. In *40th International Conference on Environmental Systems* (p. 6024).
- [9]. Horányi, M., Szalay, J., Kempf, S., Schmidt, J., Grün, E., Srama, R., & Sternovsky, Z. (2015). A permanent, asymmetric dust cloud around the Moon. *Nature*, 522(7556), 324-326.
- [10]. Wagner, S. (2006). *The Apollo Experience Lessons Learned for Constellation Lunar Dust Management*. NASA/TP-2006- 213726
- [11]. Horanyi, M., Walch, B., Robertson, S., & Alexander, D. (1998). Electrostatic charging properties of Apollo 17 lunar dust. *Journal of Geophysical Research: Planets*, 103(E4), 8575–8580.
- [12]. Berg, O., Wolf, H., & Rhee, J., Lunar soil movement registered by the Apollo 17 cosmic dust experiment, in *Interplanetary Dust and Zodiacal Light*, Elsasser, H. and Fechtig, H., Eds., New York: Springer-Verlag, 1976, pp. 233–237.
- [13]. Grün, E. & Horányi, M. (2013). A new look at Apollo 17 LEAM data: Nighttime dust activity in 1976. *Planetary and Space Science*, 89, 2-14..
- [14]. Berg, O., Wolf, H., & Rhee, J.(1976). Lunar soil movement registered by the Apollo 17 cosmic dust experiment, In *Interplanetary Dust and Zodiacal Light*, Elsasser, H. and Fechtig, H., Eds., New York: Springer-Verlag, , pp. 233–237.
- [16]. Liu, Y., Park, J., Hill, E., Kihm, K., & Taylor, L. (2006). Morphology and physical characteristics of Apollo 17 dust particles. In *Earth & Space 2006: Engineering, Construction, and Operations in Challenging Environment*, 1-6.
- [17]. Rosenfeld, E. & Zakharov, A. (2016). Role of stochastic processes in particle charging due to photoeffect on the Moon. *arXiv preprint arXiv:1611.0081*.
- [18]. Mishra, S. & Bhardwaj, A. (2019). Photoelectron sheath on lunar sunlit regolith and dust levitation. *The Astrophysical Journal*, 884(1), 5.
- [19]. Jordan, A., Stubbs, T., Wilson, J., Schwadron, N., Spence, H., & Joyce, C. (2014). Deep dielectric charging of regolith within the Moon's permanently shadowed regions. *Journal of Geophysical Research: Planets*, 119(8), 1806-1821.].
- [20]. Whipple E. (1981). *Rep. Prog. Phys.* 44,1197.
- [21]. Olhoef, G. & Strangway, D. (1975). Dielectric properties of the first 100 meters of the Moon. *Earth and Planetary Science Letters*, 24(3), 394-404.
- [22]. De, B. & Criswell, D. (1977). Intense localized photoelectric charging in the lunar sunset terminator region, 1. Development of potentials and fields. *Journal of Geophysical Research*, 82(7), 999-1004.
- [23]. Criswell, D. (1973). Horizon-glow and the motion of lunar dust. In *Photon and particle interactions with surfaces in space* (pp. 545-556). Springer, Dordrecht.
- [24]. Singer, S. & Walker, E.(1962). Electrostatic dust transport on the lunar surface. *Icarus*, 1(1-6), 112-120..
- [25]. Park, J., Liu, Y., Kihm, K., & Taylor, L.(2008). Characterization of lunar dust for toxicological studies. I: Particle size distribution. *Journal of Aerospace Engineering*, 21(4), 266-271.
- [26]. Wallace, W., Phillips, C., Jeevarajan, A., Chen, B., & Taylor, L. (2010). Nanophase iron-enhanced chemical reactivity of ground lunar soil. *Earth and Planetary Science Letters*, 295(3-4), 571-577.
- [27]. Belvin, W. & Watson, J. (2006). *Structural concepts and materials for lunar exploration habitats*.
- [28]. NASA Engineering and Safety Center, Crew Exploration Vehicle, “Smart Buyer” Design Team Final Report, May 2006
- [29]. Wilson, J., Miller, J., Konradi, A. & Cucinotta, F. (1997). Shielding strategies for human space exploration, NASA CP 3360.
- [30]. Benaroya, H. (2005). Multiple-Customer Industrial/Scientific/Exploration Facility, LEAG Conference on Lunar Exploration 2005, Houston TX, Oct. 27, 2005.
- [31]. Naito, M., Kitamura, H., Koike, M., Kusano, H., Kusumoto, T., Uchihori, Y., ... & Kodaira, S. (2021). Applicability of composite materials for space radiation shielding of spacecraft. *Life sciences in space research*, 31, 71-79.
- [32]. Yao, C., Qi, Z., Chen, W., & Zhang, C. (2021). Experimental study on CF/PEEK thermoplastic fastener: Effects of fastener matrix crystallinity and fibre content on the strength of single-lap joint. *Composites Part B: Engineering*, 213, 108737.
- [33]. Naito, M., Kitamura, H., Koike, M., Kusano, H., Kusumoto, T., Uchihori, Y., ... & Kodaira, S. (2021). Applicability of composite materials for space radiation shielding of spacecraft. *Life sciences in space research*, 31, 71-79.
- [34]. Weiss, P. et al. (2020). Advanced materials for future lunar extravehicular activity space suit. *Advanced Materials Technologies*, 5
- [35]. Harrison, C, Weaver, S, Bertelsen, C, Burgett, E, Hertel, N, et al. (2008). Polyethylene/boron nitride composites for space radiation shielding. *Journal of Applied Polymer Science* 109(4), 2529–2538.
- [36]. Chen H, Chen Y, Li CP, Zhang H, Williams JS, et al. (2007). Eu-doped Boron Nitride Nanotubes as a Nanometer-Sized Visible-Light Source. *Advanced Materials* 19(14),1845-1848.
- [37]. Golberg, D., Bando, Y., Tang, C., & Zhi, C. (2007). Boron nitride nanotubes. *Advanced Materials* 19(18), 2413–2432.

- [38]. Walton, O. (2007). *Adhesion of Lunar Dust*, NASA/CR—2007-214685. Retrieved from nasa.gov.
- [39]. Whipple, E. (1981). Potentials of surfaces in space, *Rep. Prog. Phys.*, 44, 1197–1250.
- [40]. Walton, O. (2007). Adhesion of Lunar Dust, NASA/CR—2007-214685. Retrieved from nasa.gov
- [41]. Walton, O. (2007). Adhesion of Lunar Dust, NASA/CR—2007-214685. Retrieved from nasa.gov